conductivity of the $LiNO_3$–$NaNO_3$ system was also studied.

Glossary

a	radius of the heating element (outer diameter of the capillary), m
I	current, A
k	thermal diffusivity, m^2/s
I_e	instrument constant
q	heat generated at the unit length of the heater, W/m
R	electrical resistance, Ω
S	electrical resistance, Ω
t	time, s
T	temperature, K
ΔV	unbalanced voltage, V
λ	thermal conductivity, W/(m·K)

Registry No. $LiNO_3$, 7790-69-4; $NaNO_3$, 7631-99-4; KNO_3, 7757-79-1; $NaNO_2$, 7632-00-0.

Literature Cited

(1) Nagasaka, Y.; Nagashima, A. *Ind. Eng. Chem. Fundam.* **1981**, *20*, 216.
(2) Hoshi, M.; Omotani, T.; Nagashima, A. *Rev. Sci. Instrum.* **1981**, *52*, 755.
(3) Omotani, T.; Nagasaka, Y.; Nagashima, A. *Int. J. Thermophys.* **1982**, *3*, 17.
(4) Turnbull, A. G. *Aust. J. Appl. Sci.* **1961**, *12*, 30.
(5) Odawara, O.; Okada, I.; Kawamura, K. *J. Chem. Eng. Data* **1977**, *22*, 222.
(6) Vargaftik, N. V. *Izv. VTI* **1952**, *21*, 1.
(7) National Engineering Lab, "Liquid Thermal Conductivity—A Data Survey to 1973"; Her Majesty's Stationary Office: Scotland, 1975.
(8) Cooke, J. W. Report ORNL-4831; Oak Ridge National Laboratory: Oak Ridge, TN, 1973.
(9) Gustafsson, S. E.; Halling, N. O.; Kjellander, R. A. E. *Z. Naturforsch. A* **1968**, *23*, 682.
(10) Mcdonald, J.; Davis, H. T. *J. Phys. Chem.* **1970**, *74*, 725.
(11) White, L. R.; Davis, H. T. *J. Chem. Phys.* **1967**, *47*, 5433.

Redox Electromotive Force Measurements in the Molten CuCl–CuCl2 System and Thermodynamic Properties of Liquid CuCl2. 1

Zafirios Glazitzoglou

Lehrstuhl für Technische Thermodynamik an der RWTH Aachen, 5100 Aachen, Federal Republic of Germany

Cu(I)/Cu(II) redox electromotive force measurements in the molten binary system CuCl–CuCl2 were carried out by using a chlorine/chloride reference electrode in a temperature range from about 400 to 530 °C and for several concentrations up to 10 mol % CuCl2. The free energy, enthalpy, and entropy change of the reaction $CuCl(l) + \frac{1}{2}Cl_2(g) = CuCl_2(l)$, as well as the unknown thermodynamic properties of molten solute CuCl2, have been calculated as a function of temperature.

Introduction

No thermodynamic properties of pure molten $CuCl_2$ are included in the known collected thermodynamic data, such as in ref *1–4*. The reason is that $CuCl_2$ cannot exist in the pure fused state because of its decomposition already at the solid phase (*5, 6*). Even the melting point values of $CuCl_2$ given in the literature differ widely between 498 and 633 °C (*4, 6–8*).

The calculation of excess thermodynamic properties, as well as of activity coefficients, in a molten mixture requires the definition of a reference standard state for each liquid component. The purpose of the present work is to obtain experimentally the data necessary for the thermodynamic description of liquid cupric chloride. These investigations are part of an extensive study in order to determine the thermodynamic properties of the quaternary molten system $CuCl$–$CuCl_2$–KCl–$LiCl$ by means of emf measurements.

The present study is the first in which redox potentials in the molten $CuCl$–$CuCl_2$ system were measured. Because of the volatility of the melt and the $CuCl_2$ decomposition, measurements have been made only up to 10 mol % $CuCl_2$. The heat capacity, the Gibbs energy, the entropy, the enthalpy, and the formation potential of molten solute $CuCl_2$ as well as the enthalpy and entropy of fusion were calculated from the data obtained.

The results can be used to estimate the thermodynamic quantities of several chemical processes in which copper chloride melts act as a reactant or catalyst. Among such thermodynamic calculations are, for example, reaction conversions for the chlorination of methane or other hydrocarbons (*7, 9*), potentials for the electrolysis of molten cuprous chloride (*10*), equilibrium chlorine pressures, and the heat requirement for the chlorine production from cupric chloride (*7–9*).

Further, a knowledge of the Cu(I)/Cu(II) redox potentials in molten copper chloride mixtures is of significant importance in the understanding of the structure of these melts (*8*).

Experimental Section

The following electrochemical cell was used:

$$\ominus \; C \; \big| \; CuCl-CuCl_2(l) \; \big| \; KCl-LiCl(l) \; \big| \; Cl_2(g), \; C \; \oplus$$

A diagram of this quartz cell is shown in Figure 1. A graphite rod surrounded by a quartz glass tube served as an indicator redox electrode. The chlorine–chloride reference electrode used (*11*) consists of a graphite tube immersed in molten KCl–LiCl eutectic (41.5 mol % KCl). Chlorine was bubbled through the melt. An asbestos diaphragm with a resistance of about 8000 Ω separates the two electrode compartments. The melt was contained in a quartz glass crucible. The temperature was measured with a calibrated NiCr–Ni thermocouple surrounded by a sheath of quartz glass. Cuprous chloride (Merck Darmstadt, FRG, No. 2739 p.a. minimum 98%) was dried under vacuum (10^{-3} mmHg) at 100 °C for 24 h to remove the main part of the moisture and then at 150 °C for a further 24 h. The eutectic (KCl Merck 4936 p.a. minimum 99.5%, LiCl Merck 5679 p.a. minimum 99%) was prepared according to the procedure described in ref *12* by melting under anhydrous HCl. Cupric chloride (Ventron Karlsruhe, FRG, No. 88759, anhydrous) was used directly. Chlorine (Linde Höllriegelskreuth, FRG,
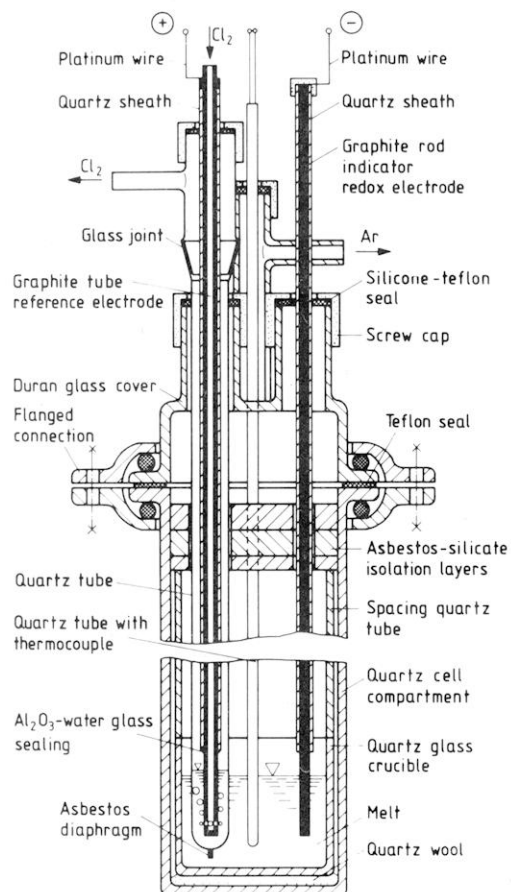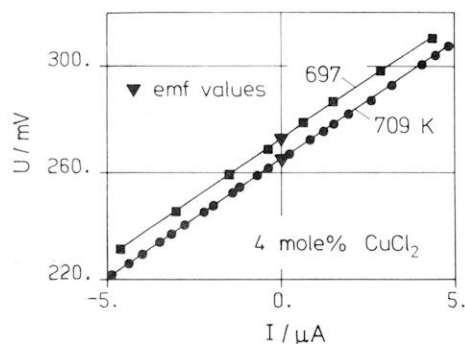
Figure 1. Diagram of the electrochemical cell.

Figure 2. Reversibility test of the applied cell. Measured voltage–current curves at 4 mol % $CuCl_2$.

minimum 99.8%) was dried by bubbling through concentrated sulfuric acid.

Results and Discussion

Reversible working electrodes are required to achieve correct emf measurements. In order to test for reversibility, the cell potential was over- and undercompensated by using an antiparallel coupling controlled dc voltage source. The measured voltage–current curves are continuous and nearly linear and possess no hysteresis (Figure 2), thus indicating the reversible working of the electrochemical cell. The emf measurements were performed practically currentless (10^{-7} A) by using a high-impedance voltmeter (10^7 Ω).

Cell potentials are corrected for the thermoelectric emf produced due to the different temperature of the platinum wire electrode contacts. These forces were measured separately as a function of temperature for the arrangement used and may be expressed by the equation

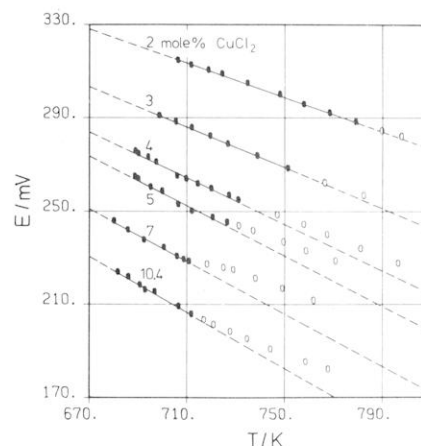$$E_t/mV = -1.94 + 0.0023T + 498/T \qquad (1)$$

Figure 3. Plots of emf measurements: fitted data (●) and their least-squares lines vs. temperature at the experimental concentrations investigated.

Table I. Least-Squares Lines of the Cu(I)/Cu(II) Redox Emf Measurements (E/mV) at Various Mole Fractions of $CuCl_2$ (x_2) as a Function of the Thermodynamic Temperature (T/K)

x_2	E/mV	x_2	E/mV
0.0202	$574.1 - 0.3673T$	0.0500	$633.2 - 0.5363T$
0.0300	$592.5 - 0.4317T$	0.0700	$624.4 - 0.5579T$
0.0401	$616.6 - 0.4961T$	0.1042	$629.8 - 0.5960T$

where T/K is the thermodynamic temperature. Using the chlorine pressures of the reference electrode, measured with an accuracy of about 4 mbar, we converted all data to the standard pressure of 1 atm = 1.01325 bar. The results, shown in Figure 3, are plotted vs. temperature for the experimental concentrations investigated. In the lower temperature range the relationship between emf measurements and temperature is linear, which is typical for molten salts. By stirring the melt vigorously, stable emf values could be obtained in 30–40 min. With rising temperature the curves deviate from linearity, and in the time mentioned above the emf values start slowly increasing. This behavior is due to the change in composition of the copper chlorides melt caused by the beginning volatilization and later by the cupric chloride decomposition. This temperature range, at which the emf measurements start being instable, depends on the concentration and was confirmed by a simultaneous DSC-TG thermoanalysis (TA 2000 C Mettler, CH, quartz crucible, 20 K min^{-1}, 100 mL min^{-1} N$_2$) for two chosen concentrations. In the case of 2 mol % $CuCl_2$ a temperature of about 510 °C was determined for a considerable volatilization (0.5 wt % of the sample) and 540 °C for a chlorine evolution from the melt; at 7 mol % $CuCl_2$ the temperatures were 460 and 480 °C, respectively. Only the stable measurements, marked by full circles in Figure 3, are considered for a linear correlation of the data points. The results may be expressed by the equations shown in Table I. The average absolute deviation is 0.48 mV and the relative 0.19%. The emf measurements for the investigated reaction

$$CuCl(l) + {}^1/_2Cl_2(g) = CuCl_2(l) \qquad (2)$$

may be expressed by

$$E = -\frac{1}{F}\left(\Delta^R G°(T) + 2.303RT \log \frac{x_2}{x_1} + 2.303RT \log \frac{f_2}{f_1}\right) \qquad (3)$$

where $\Delta^R G°$ is the standard (pure substances at 1 atm) molar free energy change of the reaction, $F = 96.487$ J mV^{-1} mol^{-1} is the Faraday constant, $R = 8.31433$ J mol^{-1} K^{-1} is the gas constant, T is the thermodynamic temperature, x_i is the mole
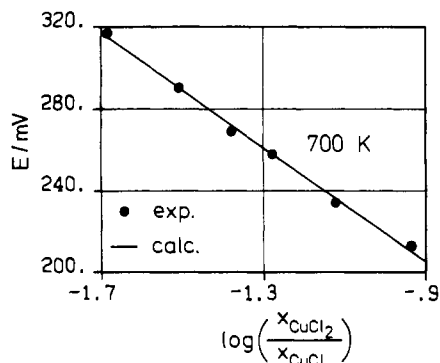
Figure 4. Comparison of emf measurements ($\bullet$) with theoretical values (—) calculated for f_2/f_1 = constant at 700 K and various concentrations.

Figure 5. Comparison of measured and calculated data for the standard free energy change of the reaction $CuCl(l) + \frac{1}{2}Cl_2(g) = CuCl_2(l)$.

fraction (CuCl: i = 1; $CuCl_2$: i = 2), and f_i is the corresponding activity coefficient.

When the emf measurements are plotted against the term log (x_2/x_1) at a constant temperature, the results are represented well by straight lines, as shown in Figure 4 for the data obtained at 700 K. The gradient of the experimental regression line is −139.7 mV, practically identical with the theoretical value (see eq 3) $-2.303RT/F$ = −138.9 mV. This indicates that at a constant temperature the activity coefficients of the copper chlorides are either unity ($f_1 = f_2 = 1$ according to an ideal mixture) or their ratio is constant within the concentration range investigated. Thus, it follows from eq 3 that

$$\Delta^R G^\infty(T) = \Delta^R G^\circ(T) + 2.303RT \log\left(\frac{f_2}{f_1}\right)^\infty =$$

$$\text{constant at } T = \text{constant} \quad (4)$$

where $\Delta^R G^\infty$ is the standard free energy change of the reaction (eq 2) in the dilute $CuCl_2$ liquid mixture at 1 atm and where the superscript ∞ denotes this standard state. The following expression was derived for the unknown $\Delta^R G^\infty$ by using the heat capacity values for CuCl(l) and $Cl_2(g)$ reported in ref *3*:

$$\Delta^R G^\infty/(\text{kJ mol}^{-1}) = -\int\int \frac{\Delta^R C_p}{T} dT^2 =$$

$$a + bT + cT \ln T + (0.063 \times 10^{-6})T^2 - 71.13/T \quad (5)$$

However, a plot of the experimental $\Delta^R G^\infty$ values vs. temperature, obtained by the present emf data using eq 3 and 4, indicates a sufficient linear behavior for $\Delta^R G^\infty$ in the temperature range investigated, as shown in Figure 5. A least-squares treatment of the stable emf data yielded

$$\Delta^R G^\infty/(\text{kJ mol}^{-1}) =$$

$$-54.36 + (66.73 \times 10^{-3})T + (0.063 \times 10^{-6})T^2 - 71.13/T \quad (6)$$

where T/K is the thermodynamic temperature. The average absolute deviation is 0.21 kJ mol^{-1} and the relative 3.2%. The data points of the instable emf measurements (compare Figure 3), not used for the least-squares correlation, are also plotted in Figure 5. Even in this case a maximal deviation of less than 0.5 kJ mol^{-1} is observed. Thus, a high accuracy may be expected for the obtained $\Delta^R G^\infty$ values. Besides the results are in good agreement with the data calculated in ref *8*, assuming an ideal mixture, using equilibrium chlorine pressures above the present molten system measured in almost the same temperature range and at concentrations up to 30 mol % $CuCl_2$ (Figure 5). Deviations, as shown in Figure 5, arise often between data obtained by different experimental methods and are within the accuracy tolerance given in ref *8*.

Using the well-known thermodynamic relations, one can calculate the standard entropy change of the reaction (eq 2)
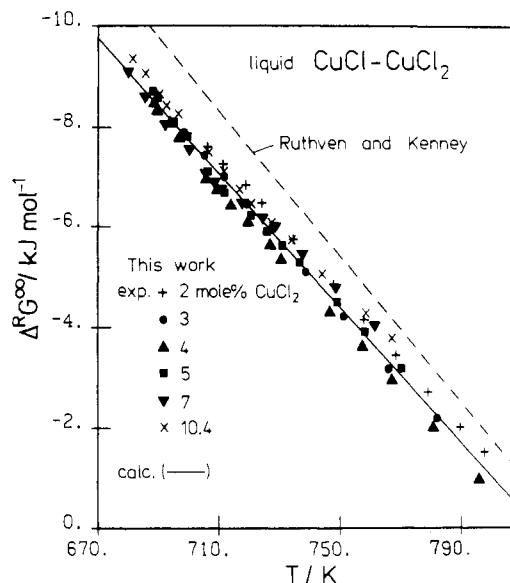
in dilute $CuCl_2$ liquid mixture $\Delta^R S^\infty$, and the standard enthalpy change $\Delta^R H^\infty$, from eq 6. Thus

$$\Delta^R S^\infty/(\text{J mol}^{-1} \text{ K}^{-1}) =$$

$$-66.73 - (0.126 \times 10^{-3})T - (71.13 \times 10^3)T^{-2} \quad (7)$$

$$\Delta^R H^\infty/(\text{kJ mol}^{-1}) = -54.36 - (0.063 \times 10^{-6})T^2 - 142.26/T \quad (8)$$

It follows from eq 4 for the Gibbs energy of solute liquid cupric chloride defined by

$$G^\infty_{CuCl_2(l)} = G^\circ_{CuCl_2(l)} + RT \ln\left(\frac{f_{CuCl_2}}{f_{CuCl}}\right)^\infty \quad (9)$$

that

$$G^\infty_{CuCl_2(l)} = \Delta^R G^\infty + G^\circ_{CuCl(l)} + 0.5G^\circ_{Cl_2(g)} \quad (10)$$

where the superscript $^\circ$ denotes "pure" and ∞ denotes "dilute". Thus, it holds $G^\infty_{CuCl_2(l)} = G^\circ_{CuCl_2(l)}$, only when the molten system can be treated as an ideal mixture ($f_{CuCl} = f_{CuCl_2} = 1$).

Using literature data (*3*), we derived the free energy G^∞, the entropy S^∞, the enthalpy H^∞, and the heat capacity C_p^∞ of liquid solute $CuCl_2$ in the molten $CuCl-CuCl_2$ mixture from eq 6 and 10:

$$G^\infty/(\text{kJ mol}^{-1}) =$$

$$-212.67 + (436.86 \times 10^{-3})T - (85.4 \times 10^{-3})T \ln T$$

$$S^\infty/(\text{J mol}^{-1} \text{ K}^{-1}) = -351.46 + 85.4 \ln T$$

$$H^\infty/(\text{kJ mol}^{-1}) = -212.67 + (85.4 \times 10^{-3})T$$

$$C_p^\infty = 85.4 \text{ J mol}^{-1} \text{ K}^{-1} \quad (11)$$

The melting point T_m = 903 K reported in ref *6* was used to calculate the enthalpy and the entropy of fusion:

$$\Delta^m H^\infty = 23.13 \text{ kJ mol}^{-1} \qquad \Delta^m S^\infty = 25.6 \text{ J mol}^{-1} \text{ K}^{-1} \quad (12)$$

Further, the present results were applied to calculate the unknown standard formation potential of molten $CuCl_2$, according to the reaction

$$Cu(s) + Cl_2(g) = CuCl_2(l) \quad (13)$$

This emf cannot be determined directly by emf measurements because of the $CuCl_2$ decomposition and its spontaneous re-

acting with the copper electrode. The equation obtained is

$$E^{\infty}/mV = 1003.6 - 1.5075T + 0.1340T \ln T -$$
$$(16.9 \times 10^{-6})T^2 + 737.2/T \quad (14)$$

Similarly, on the basis of the above data, the thermodynamic quantities of other reactions involving copper chloride melts and the excess properties of these multicomponent mixtures could be evaluated. However, it must be remarked that all these data should be used only within the concentration range investigated and that extrapolations are only then accurate if the molten system $CuCl$–$CuCl_2$ can be treated as an ideal mixture at the concerning concentrations.

Acknowledgment

I thank T. Ritterbex for his help in carrying out the experimental work.

Registry No. $CuCl_2$, 7447-39-4; $CuCl$, 7758-89-6.

Literature Cited

(1) Chase, M. W., Jr.; Curnutt, J. L.; Downey, J. R., Jr.; McDonald, R. A.; Syverud, A. N.; Valenzuela, E. A. "JANAF Thermochemical Tables, 1982 Supplement"; *J. Phys. Chem. Ref. Data* **1982**, *11*, 695.
(2) Wicks, C. E.; Block, F. E. "The Thermodynamic Properties of 65 Elements, Their Oxides, Halides, Carbides and Nitrides"; U.S. Government Printing Office: Washington, DC, 1963; *Bull.—U.S., Bur. Mines*, No. 605.
(3) Barin, I.; Knacke, O. "Thermochemical Properties of Inorganic Substances"; Springer-Verlag: West Berlin, 1973.
(4) Janz, G. J. "Molten Salt Handbook"; Academic Press: New York, 1967.
(5) Hammer, R. R.; Gregory, N. W. *J. Phys. Chem.* **1964**, *68*, 3229.
(6) Biltz, W.; Fischer, W. *Z. Anorg. Allg. Chem.* **1927**, *166*, 290.
(7) Fontana, C. M.; Gorin, E.; Kidder, G. A.; Meredith, C. S. *Ind. Eng. Chem.* **1952**, *44*, 363.
(8) Ruthven, D. M.; Kenney, C. N. *J. Inorg. Nucl. Chem.* **1968**, *30*, 931.
(9) Sundermeyer, W. *Angew. Chem.* **1965**, *77*, 241.
(10) Drossbach, P. *Z. Elektrochem.* **1952**, *56*, 23.
(11) Giazitzoglou, Z. *Ber. Bunsenges. Phys. Chem.* **1982**, *86*, 894.
(12) Giazitzoglou, Z. *Electrochim. Acta* **1963**, *28*, 491.

Thermal Diffusion Factors near the Azeotrope Conditions of Ethanol–Water Mixtures

Edward R. Peterson, Tevin Vongvanich, and Richard L. Rowley*

Department of Chemical Engineering, Rice University, Houston, Texas 77251

A thermal diffusion column has been designed with unique sampling capabilities. This column has been used to Investigate the behavior of the thermal diffusion factor, the thermal diffusion coefficient, and the corresponding Onsager coefficient in the azeotropic region of ethanol–water mixtures. In particular, the temperature dependence of these coefficients has been studied at 1 atm between 29 and 76 °C, to within 2 °C of the azeotrope point. Within statistical justification of the data, all three coefficients are linear. Experimental error increases near the azeotrope point, but it appears that no anomalous behavior due to azeotropic point proximity occurs; therefore, effective resolution of azeotropic mixtures can be made with thermogravitational techniques alone or in conjunction with distillation columns.

Introduction

Thermal diffusion factors, α_i, determine the magnitude of separations achieved at steady state by an applied temperature gradient. While thermal diffusion separations of liquid mixtures are not widely employed on a commercial scale due to the size of α_i, there are important thermophysical property regions where thermal diffusion data may take on increased commercial significance and play an important role in elucidating the nature of liquid mixture interactions and resultant transport phenomena. For example, it has been shown that the thermal diffusion factor exhibits a "critical anomaly" or diverges as the temperature of a binary mixture approaches its liquid–liquid critical point or consolute temperature (1–4). Experiments indicate that this is due to the rapid decrease in magnitude of the diffusion coefficient thereby decreasing back-diffusion and enhancing dramatically the steady-state separation (3, 4). Similarly, near an azeotrope point, thermal diffusion data may

have an anomalous temperature dependence which would affect separations. Thermal diffusion could find application in conjunction with distillation columns, using the thermogravitational column to break the azeotrope (5). We report here the behavior of the thermal diffusion factor in ethanol–water mixtures of azeotrope composition as the temperature is increased to the azeotrope point.

Experimental Section

Horne and Bearman (6, 7) have shown that thermal diffusion factors can be obtained from thermogravitational columns by measuring steady-state separations using the equations

$$\alpha_1 = ABT\beta\Delta w_1 / [w_1 w_2 (1 - F)] \quad (1)$$

$$F = 19AB\rho(\bar{V}_2 - \bar{V}_1)\Delta w_1 / 1430 \quad (2)$$

$$B = \rho/\eta D \quad (3)$$

where A is a well-defined apparatus constant, w_i is the mass fraction of component i, Δw_i is the steady-state composition difference between the top and the bottom of the column, $\bar{V}_i$ is the partial specific volume of species i, ρ is the density, η is the shear viscosity, and D is the mutual diffusion coefficient. Stanford and Beyerlein (8) have shown that thermogravitational columns without end reservoirs eliminate most end-effect problems and constitute an accurate reproducible means of determining thermal diffusion factors.

The column used in this work is shown schematically in Figure 1; the top seal, the sample tube arrangement, the column spacer, the vent, and the thermocouple wells are detailed in Figure 2. The column was made from three pieces of stainless-steel tubes of nominal o.d.'s and wall thicknesses 0.990, 1.135, 1.615 and 0.160, 0.187, and 0.175 in., respectively. After machining and straightening, this resulted in a